ELSEVIER

Surface Science 423 (1999) 90–98

surface science

TDS study of the bonding of CO and NO to vacuum-cleaved NiO(100)

R. Wichtendahl, M. Rodriguez-Rodrigo, U. Härtel, H. Kuhlenbeck*, H.-J. Freund

Fritz-Haber-Institut der Max-Planck-Gesellschaft, Abteilung Chemische Physik, Faradayweg 4–6, Berlin D-14195, Germany

Received 27 August 1998; accepted for publication 24 November 1998

Abstract

Using thermal desorption spectroscopy (TDS) we have determined the adsorption enthalpies of NO and CO on a NiO(100) surface obtained by cleavage of a NiO single crystal rod under ultra-high vacuum (UHV) conditions. The TDS data have been evaluated using the leading edge method and complete analysis, yielding values of 0.30 ± 0.04 and 0.57 ± 0.04 eV for the heats of adsorption of CO and NO, respectively, in the low coverage regime. These values decrease with increasing coverage down to the respective multilayer values. The results obtained experimentally are different from the theoretical ones, in that the experimental values are systematically larger. This is possibly due to the influence of the Ni3d electrons as concluded from a comparison with TDS data for CO on vacuum-cleaved MgO(100). The adsorbate bonding energies obtained for vacuum-cleaved NiO(100) are in good agreement with values for thin NiO(100) films deduced from thermal-desorption studies and infrared investigations.

Keywords: CO; TDS; Thermal desorption spectroscopy; Vacuum cleaved NiO(100)

1. Introduction

Although CO and NO on NiO(100) are seemingly simple adsorption systems, the description of the adsorbate–substrate bonds is still under debate. In particular, the theoretically predicted adsorption energies of CO and NO are at variance with experimental data. Pacchioni and Bagus calculated on the SCF-level a CO–NiO(100) bonding energy of 0.24 eV [1], which is not far from the experimental results presented in this paper. However, this result was obtained on the Hartree–Fock level without correction for the basis set superposition error (BSSE). The latter tends to decrease the calculated bonding energy. Pöhlchen and Staemmler obtained values between 0.03 and 0.1 eV [2] using different ab initio methods, carefully corrected for the BSSE. Nygren and Pettersson [3] noted that with increasing cluster size and sophistication of the theoretical methods the results tend to get smaller. The situation for NO/NiO(100) is similar in that the theoretical results are smaller than the published experimental ones. According to Pöhlchen, the adsorption energy should not be larger than 0.23 eV [4] and in Refs. [5] and [6] a value of about 0.1 eV was reported. More recent calculations employing large basis sets and clusters point toward a bonding energy which is near to zero [7]. Published experi-

* Corresponding author. Fax: +49-30-8413-4307; e-mail: Kuhlenbeck@FHI-Berlin.MPG.DE.

0039-6028/99/$ – see front matter
PII: S0039-6028(98)00915-7

mental data are ≈ 0.32 eV and 0.43 eV for CO [8,9] and 0.52 eV for NO [5].

Up to now, only TDS data for CO adsorption on thin NiO(100) films were available in the literature [8,9]. For NO, TDS data for a UHV-cleaved NiO(100) single crystal substrate have been published [5]. Also, thin-film data are available [5].

Despite tremendous theoretical effort, the contradiction between experimental and theoretical results could not be resolved. Therefore, the idea arose that, especially for CO, the limited quality of thin films grown by oxidation might be responsible for the discrepancy between theoretical and experimental results. It was argued that the published experimental results might be due to adsorption on defects [3]. A similar argument was put forward for CO adsorption on MgO(100), where also the experimental results differed from the theoretical ones. Therefore we have set up a TDS experiment which permits scanning of the temperature in the range between $T = 20$ K and 400 K using NiO(100) single crystals cleaved in UHV as substrates for the respective adsorbate. The high quality of NiO(100) surfaces prepared by cleavage in UHV renders defect adsorption a negligible effect. Thus we hope that the bonding energies determined represent a final result. Experiments for CO and NO adsorption on MgO(100) are presently being carried out, and we refer to some aspects in this paper. Details will be presented elsewhere.

2. Experimental

The substrates used for the TDS experiments were [100]-oriented single crystal cylinders with a diameter of 1 cm and a length of about 3 cm obtained from Kepin in Leimen, Germany. These were mounted to a helium-cooled cold finger as depicted in Fig. 1.

The sample was pressed onto the cold finger using a stainless-steel plate which was contacted to the sample via two slits in the NiO rod. A tantalum filament wrapped around the lower end of the NiO cylinder was used for heating purposes. The thermocouple was anchored to the sample by

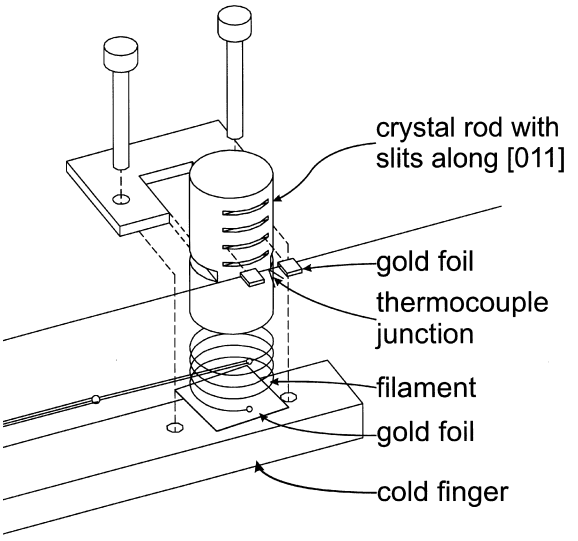

Fig. 1. Sample setup used for the TDS experiments.

two pieces of gold foil. These were pressed into a slit in the rod so that the thermojunction was free hanging. Then the slit was filled with glue (Torrseal, Varian) so that the heat contact to the sample was maintained by the glue and the pieces of gold foil (via the NiCr/Cr wire). The rod was cleaved along its (100) plane with two blades guided by slits in the rod along [011]. With this setup, heating rates of up to 2 K/s could be realized. After cleavage, the surfaces obtained could be used for several days; the desorption spectra were fully reproducible during this time. In order not to damage the cleaved surfaces, exposure to ion or electron beams was avoided. LEED, which was performed after the TDS experiments, displayed a sharp (1×1) pattern with very low background intensity up to high electron energies.

Linearity of the temperature ramp was established by a PID (proportional-integral-differential) regulator. Fig. 2 displays a typical heating-rate curve. Significant deviations ($< 10\%$) from the preset heating rate occurred only at the start of the scan. However, this is generally unavoidable since PID controllers perform damped oscillations when regulation starts. In order to achieve a stable temperature signal, the thermocouple reference junction was kept at a constant temperature of $T = 323 \pm 0.02$ K

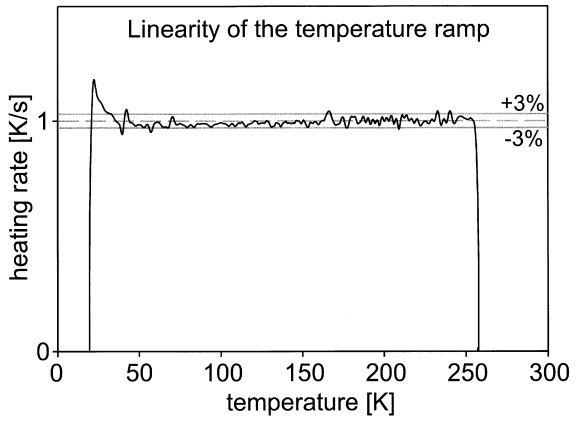

Fig. 2. Heating rate as a function of temperature for a preset heating rate of 1 K/s.

For all TDS scans, the multilayer desorption signal was found to shift by not more than ± 2 K. Deviations occurred mainly after mounting of a new sample, so they may be attributed to changed characteristics of the thermocouple. Within a set of data taken for a certain sample, the multilayer desorption temperatures did not shift by more than ± 0.3 K. In order to be able to compare data from different sets of spectra, we performed a temperature calibration as described by Schlichting and Menzel [10]. In this procedure, the desorption flux in the region of the onset of the multilayer desorption peak is compared with the flux of molecules calculated from the temperature-dependent vapor pressure of the respective molecule which was computed using heats of evaporation reported in literature (CO: 0.0885 eV; NO: 0.177 eV [10]). This method assumes a sticking probability near to one for the molecules impinging onto the condensed layer. According to Holbert et al. [11], this is fulfilled for CO and NO. As Schlichting pointed out, calibration of the temperature scale can be achieved by adding an offset to the thermovoltage of NiCr/Ni thermocouples [10]. Due to the small slope of the thermovoltage of NiCr/Ni thermocouples in the low temperature range, a temperature shift of 1 K at $T=30$ K leads to much smaller shifts at higher temperatures: 0.25 K at $T=120$ K and 0.17 K at $T=220$ K. After calibration of the temperature scale, the maxima of the CO multilayer desorption peaks were found at temperatures of around 29–30 K, depending somewhat on coverage and heating rate. For NO, multilayer desorption occurred at $T=56$ K.

Since the temperature shifts between different spectra were small, we are sure that the thermal contact of the thermocouple junction to the sample, as well the amplification electronics and the reference junction, did not introduce significant errors. This seems to be the case even for the limited heat conductivity of NiO, since the temperatures of the onsets of the multilayer desorption signals exhibited only negligible variations upon variation of the heating rate. Also shortening of the sample by cleavage did not introduce significant shifts.

For detection of the desorption signal, a Balzers QMG 112 mass spectrometer was employed. It was equipped with a so-called Feulner cup [12] consisting of an individually pumped cylindrical tube ending in a cone with a hole ($\Phi=2$ mm) at its end. In order to minimize adsorption on the inner walls of the tube, they were covered with a thin gold film. Before TDS spectra were taken, the sample was positioned in front of the hole at a distance of about 0.5 mm. This was done in order to blind out molecules desorbing from the sample holder and the side walls of the NiO rod.

Dosing was performed via a tube directed onto the sample surface, with the distance between the end of the tube and the sample being 1 mm during dosage. Therefore, the major part of the admitted gas adsorbed onto the sample surface and contamination of the sample holder was not significant. The tube was equipped with a pinhole ($\Phi=25$ μm) at the end opposite to its opening so that the pressure in the dosing system during dosage was high enough to be measured with a spinning rotor gauge. The reading of the gauge multiplied by the dosing time served as a measure for the gas dose admitted to the sample surface. Coverages have been obtained by integrating the desorption spectra. The values are proportional to the gas doses, with an error of $\pm 5\%$. All coverage values given in the following are relative to the coverage of a full monolayer which was determined from the amount of gas needed to produce first indications of a bilayer desorption peak. We note that this method is not necessarily fully appropriate,

since we cannot exclude that formation of a second layer starts before the first layer is complete. Thus a coverage of one monolayer obtained from this procedure is not necessarily equivalent to a real monolayer. We hope to obtain a more quantitative measure from LEED studies that are planned for the near future.

For comparison, TDS spectra for CO on vacuum cleaved MgO(100) are also presented. The MgO samples were single-crystal cylinders of about the same size as the NiO samples. Mounting, cleaving and recording of TDS data were performed in the same way as for the NiO(100) sample.

The pressure of the UHV system was typically in the mid 10^{-11} mbar range. During dosage it rose to, at most, 2×10^{-10} mbar.

3. Results and discussion

Figs. 3 and 4 display sets of TDS spectra for NO and CO on NiO(100) cleaved in vacuo and NiO(100) grown as a thin film on Ni(100). The thin-film data are results of earlier studies [5,8] and have been included for comparison. In the case of the thin film preparations, only cooling with liquid nitrogen was possible so temperatures below $T\approx85$ K could not be reached. Thus multilayer desorption does not show up in these data.

Obviously, the desorption spectra for the thin film NiO(100) substrates and the single-crystal samples are very similar, clearly demonstrating that the interaction of NO and CO with NiO(100) films is not dominated by defect adsorption. However, in the case of the NO adsorbate the desorption peaks are broader for the thin-film substrate than for the single-crystal substrate. This may be due partly to the higher heating rate used in the thin-film case and partly to the higher defect density of the films as compared to the cleaved surfaces. Especially the shoulders at the low and high temperature sides of the main peaks are most likely to be attributed to desorption from defect sites. For the CO adsorbate, the differences between the adsorption spectra of the thin-film substrate and the cleaved sample are less pronounced. A possible reason for this result is that

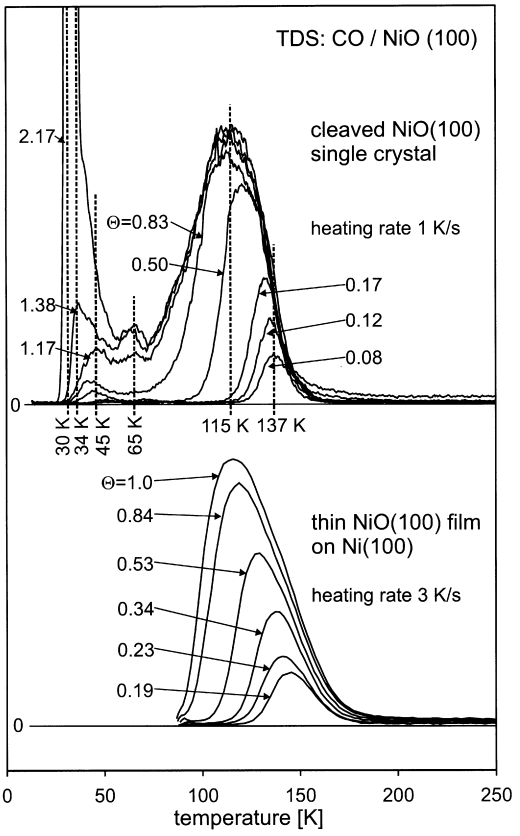

Fig. 3. Thermal desorption spectra of CO on NiO(100) cleaved in vacuo (top) and CO on a thin NiO(100) film grown by oxidation of Ni(100) (bottom). The mass spectrometer was set to mass 28 (CO). The coverages Θ are given relative to the coverage of a full monolayer.

the NO data were taken using a more defective thin film substrate. This is not unlikely, since the CO data were recorded years later when we had more experience regarding the preparation of NiO(100) films.

There are some states in the low-temperature regime of the TDS spectra of CO on cleaved NiO(100) that need to be explained in more detail: Near to the multilayer desorption peak around $T=30$ K another feature is found at $T=34$ K which we attribute to desorption of the second layer. The splitting of these features is clearly visible in Fig. 5 where these states exhibit similar intensities (the shift with respect to the features in Fig. 3 is due to a different heating rate). The

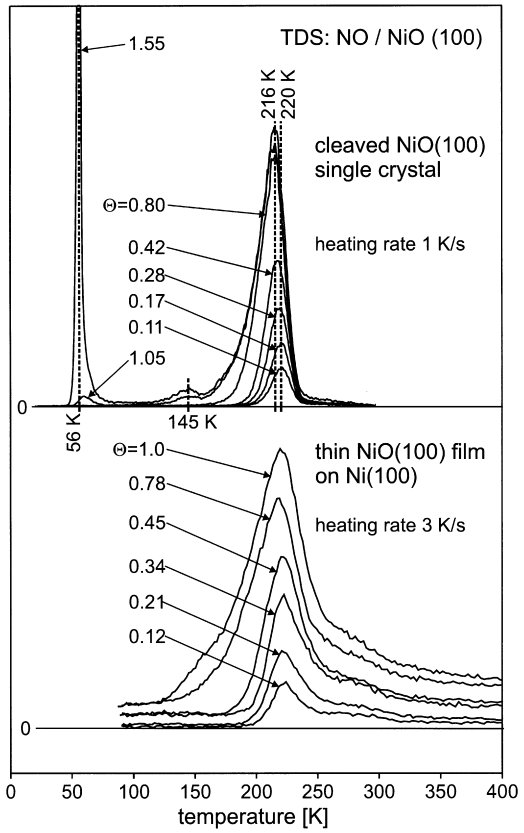

Fig. 4. Thermal desorption spectra of NO on NiO(100) cleaved in vacuo (top) and NO on a thin NiO(100) film grown by oxidation of Ni(100) (bottom). The mass spectrometer was set to mass 30 (NO). The coverages Θ are given relative to the coverage of a full monolayer.

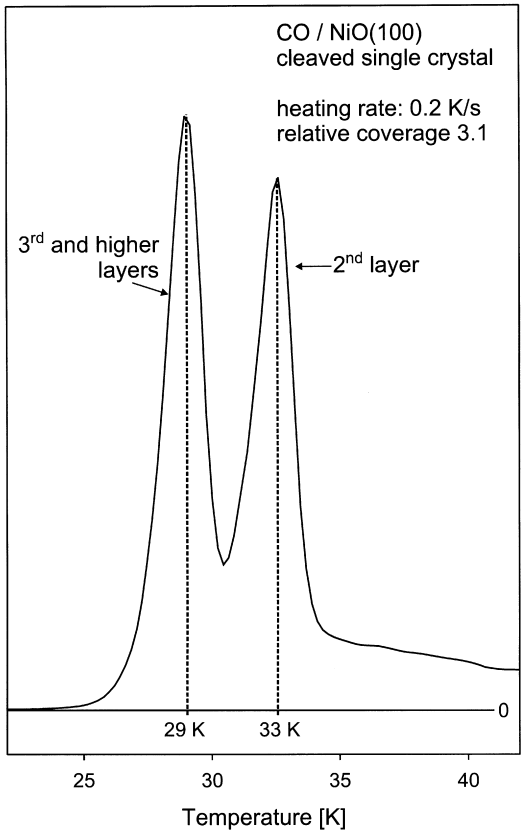

Fig. 5. Splitting of the desorption peaks of the second and the third layer of CO on cleaved NiO(100). The mass spectrometer was set to mass 28 (CO).

splittings between the desorption peaks of the third and higher layers could not be resolved. Splittings of the same type have also been observed for other adsorption systems [10].

The weak feature in the CO desorption spectra at $T=45$ K gets much stronger after ion bombardment, so it is likely to be attributed to desorption from defect sites. After heating the surface in oxygen, the original desorption spectra are retained. Therefore the state must be due to desorption from sites where oxygen ions are missing in the neighborhood. A similar explanation may hold for the peak at $T=145$ K in the NO desorption data. This state is considerably more intense in the data obtained from the thin film as compared to the cleaved substrate. Since the surface of the thin film most likely contains more defects than that of the cleaved sample, this points towards adsorption at defect sites.

A strong shift to lower temperature with increasing coverage occurs for the maxima of the (sub)monolayer desorption peaks of the CO adsorbate. A reason for this could, in principle, be that CO desorption is of second order. However, there is no obvious reason why this should be the case, since second-order desorption would imply that the interaction of two molecules is needed for desorption. A more likely reason for the shift is that it is due to repulsive lateral interactions. Also, structural phase transitions induced by the lateral interactions may be involved.

A model of the NiO(100) surface is shown in

Fig. 6. According to theory [2] and ELS data [8,13], the CO molecules bond to nickel ions at the surface. The same result was obtained for NO [5,14]. The distance between two neighboring molecules is 4.16 Å [15] when every Ni site is occupied [(1×1) structure]. At this distance, already weak direct or indirect molecule–molecule interactions come into play, which may be repulsive. If this is the case, then at low coverage a molecular arrangement with a larger nearest neighbor distance would be more favorable. This may lead to the formation of a $c(2\times2)$ superstructure with a nearest-neighbor distance of 5.88 Å which would be compressed towards a (1×1) superstructure at coverages above $\Theta=0.5$. Such a structural phase transition is compatible with the data, since especially the data of CO on the cleaved surface exhibit indications of a two-peak structure in the monolayer desorption regime between $T=75$ K and 150 K, with the low temperature peak at $T=$ 115 K being occupied at a coverage above $\Theta\approx0.5$. We note that it is not unlikely that compression beyond the (1×1) structure occurs, since a molecule–molecule distance of 4.16 Å does not give rise to strong interactions. However, in this case there are more molecules than available Ni sites on the surface, implying occupation of sites that are not centered on top of Ni ions. Molecules occupying such sites would be bound considerably more weakly to the surface. The peak at $T=65$ K in Fig. 3 may be attributed to desorption out of such a highly compressed, possibly ordered phase.

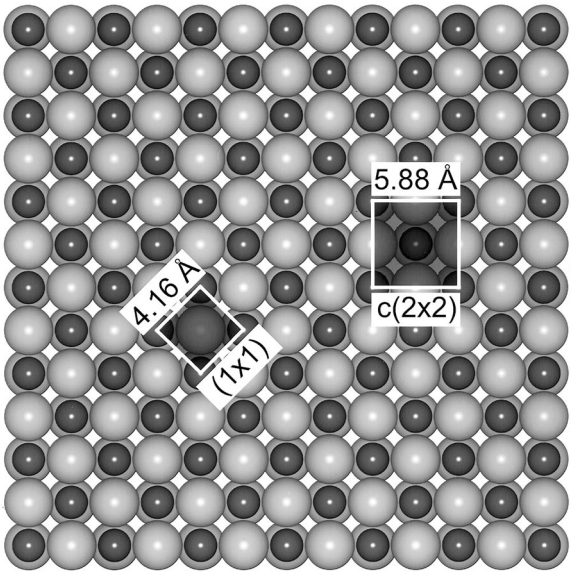

Fig. 6. Model of the NiO(100) surface. The dark spheres represent Ni ions.

For NO, the maxima of the (sub)monolayer desorption peaks do not shift significantly as a function of coverage, indicating that lateral interactions are small. However, the asymmetry of the desorption peaks, which increases with increasing coverage, points towards some kind of repulsive lateral interaction. Apparently this effect is much weaker than in the case of the CO adsorbate.

The TDS data have been quantitatively evaluated via the leading edge method and complete analysis. Details of these methods may be found in Refs. 16–18. Both methods determine the heat of adsorption of desorbing molecules as a function of the coverage of molecules on the surface. We have employed two different analysis methods for comparison. The results are displayed in Figs. 7 and 8 for CO and NO, respectively. For both types

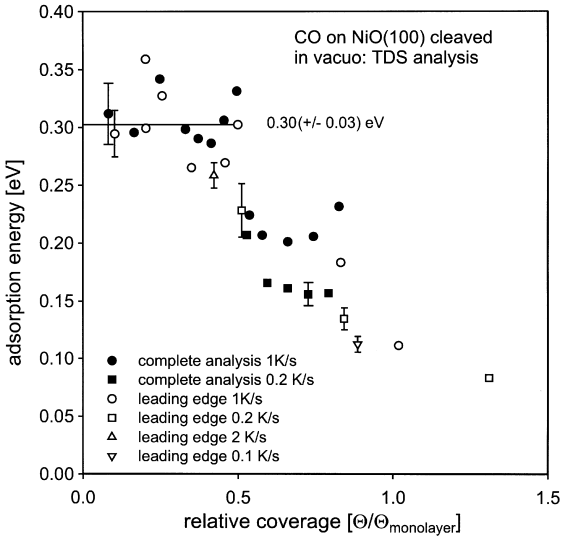

Fig. 7. Adsorption enthalpy of CO on NiO(100) cleaved in vacuo as a function of coverage. The data have been determined from TDS spectra like the ones shown in Fig. 3 (top) using the leading edge method [16] and complete analysis [17]. TDS data taken with heating rates of 0.1, 0.2, 1 and 2 K/s were used. The indicated errors were obtained from the numerical uncertainty of the fits employed in the valuation procedure.

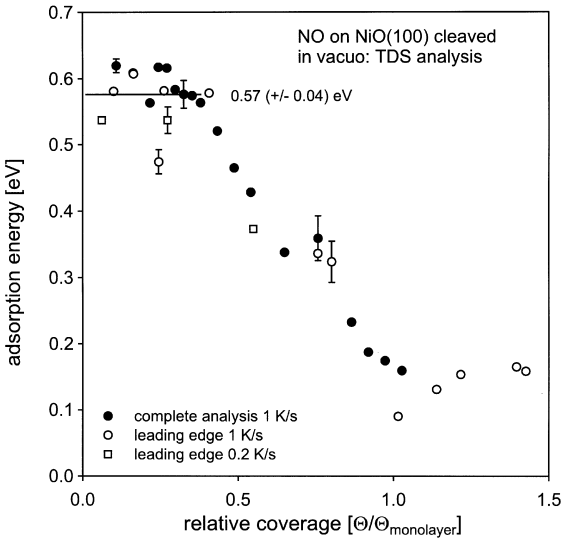

Fig. 8. Adsorption enthalpy of NO on NiO(100) cleaved in vacuo as a function of coverage. The data have been determined from TDS spectra like those shown in Fig. 4 (top) using the leading edge method [16] and complete analysis [17]. TDS data taken with heating rates of 0.2 and 1 K/s were used. The indicated errors were obtained from the numerical uncertainty of the fits employed in the evaluation procedure.

of adsorbates the data exhibit a trend already discussed in the previous paragraph: with increasing coverage the adsorption energies decrease due to lateral interactions until they reach values near to those of the respective multilayers (0.0885 eV and 0.177 eV for CO and NO, respectively [10]) at coverages of about 1. The low coverage values have been determined by averaging over the coverage regions indicated in Figs. 7 and 8, yielding values of 0.30 ± 0.03 and 0.57 ± 0.04 eV for CO and NO, respectively. These values may be compared with theoretical results, since in the low-coverage regime lateral interactions which have been neglected in the theoretical studies are weak. However, the theoretical values for CO (0.03–0.1 eV [2]) and NO (0.23 eV [4]; 0.1 eV [5,6]; near to zero [7]) seem to be systematically smaller than those of the experimental data.

The results of the ongoing studies of NO and CO adsorption on MgO(100) may be helpful for the current discussion. According to theory, the adsorption energies of CO and NO should be the same for MgO(100) and NiO(100), since the bonding should be dominated by electrostatic forces at the surface [these should be similar for NiO(100) and MgO(100)] and the d-electrons of the Ni ions in NiO(100) should not play a significant role [3]. However, according to our data the bonding of CO to MgO(100) is weaker than that to NiO(100), as demonstrated by the data displayed in Fig. 9. For small coverages, the data exhibit a desorption peak in the region around $T = 57$ K which corresponds to a bonding energy of about 0.13 eV as estimated from the Redhead equation [19]. This corresponds well to LEED results obtained by Audibert et al. [20], who observed ordered CO superstructures only at temperatures below $T = 56$ K. It also fits well to earlier

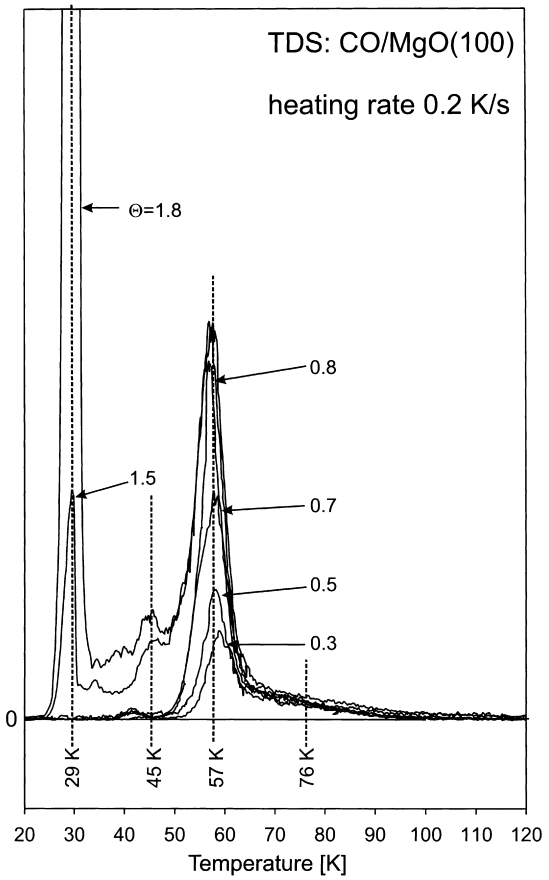

Fig. 9. Thermal desorption spectra of CO on MgO(100) cleaved in UHV. The mass spectrometer was set to mass 28 (CO). The coverages Θ are given relative to the coverage of a full monolayer.

data obtained from adsorption isotherms of CO on MgO powder, where a bonding energy of 0.15–0.17 eV was deduced [21]. The agreement with theoretical data reported by Nygren et al. (0.08 eV [3,22]) and Neyman et al. (0.11 eV [23]) is also good. However, our data compare less well with a recent calculation of Chen et al. ($E_{\mathrm{adsorption}} =$ 0.28 eV [24]). He et al. [25] reported a bonding energy of 0.43 eV for CO on a thin MgO(100) film on Mo(100). This value differs considerably from that obtained in the present study indicating that adsorption on the MgO(100) film was possibly dominated by bonding to surface defects. A reason for this result may be that the lowest accessible temperature in their experiments was $T = 80$ K so that the regular adsorption sites could not be populated. The broad feature around $T =$ 76 K in Fig. 9 is most likely due to adsorption on surface defects, since it gets much stronger after introducing additional defects by ion bombardment. This is in line with a calculated TDS spectrum [3] which exhibits desorption from step sites just at this temperature. When the evaluations and TDS measurements on CO/MgO(100) are complete, a more detailed study will be published.

For CO on cleaved MgO(100), the experimentally determined adsorption energy of 0.14 eV is not far from the theoretical values of 0.08 eV [3] and 0.22 eV [23], whereas a similar favorable comparison cannot be made for CO on NiO(100). Thus it cannot be excluded that for the bonding of NO and CO to NiO(100), also covalent interactions involving the Ni3d electrons play a role.

4. Summary

Using TDS, we have determined the adsorption energies of NO and CO on vacuum-cleaved NiO(100). The desorption spectra do not differ considerably from those obtained for thin-film substrates, indicating that thin NiO(100) films are suitable for adsorption studies. Adsorption energies of 0.30 ± 0.03 eV and 0.57 ± 0.04 eV in the low-coverage regime were obtained for CO and NO, respectively. With increasing coverage they decrease down to the values for the respective multilayers. The experimentally determined bonding energies for the low-coverage regime where lateral interaction should be weak are larger than the theoretically expected ones. As concluded from a comparison with TDS data for CO on vacuum-cleaved MgO(100), this may possibly be attributed to the influence of the Ni3d electrons onto the adsorbate–substrate interaction.

Acknowledgements

We thank Dr Thorsten Klüner and Professor L.G.M. Pettersson for valuable discussions.

References

[1] G. Pacchioni, P.S. Bagus, in: H.-J. Freund, E. Umbach (Eds.), Adsorption on Ordered Surfaces of Ionic Solids and Thin Films, Springer, Berlin, 1993, p. 180. (vol. 33 of Springer Series in Surfaces Sciences).
[2] M. Pöhlchen, V. Staemmler, J. Chem. Phys. 97 (1992) 2583.
[3] M.A. Nygren, L.G.M. Pettersson, J. Chem. Phys. 105 (1996) 9339.
[4] M. Pöhlchen, PhD thesis, Ruhr-Universität Bochum, Bochum, Germany, 1992.
[5] H. Kuhlenbeck, G. Odörfer, R. Jaeger, G. Illing, M. Menges, Th. Mull, H.-J. Freund, M. Pöhlchen, V. Staemmler, S. Witzel, C. Scharfschwerdt, K. Wennemann, T. Liedtke, M. Neumann, Phys. Rev. B 43 (1969) 1991.
[6] V. Staemmler, in: H.-J. Freund, E. Umbach (Eds.), Adsorption on Ordered Surfaces of Ionic Solid and Thin Films, Springer, Berlin, 1993, p. 169. (vol. 33 of Springer Series in Surface Sciences).
[7] T. Kluener, H.-J. Freund, private communication.
[8] D. Cappus, J. Klinkmann, H. Kuhlenbeck, H.-J. Freund, Surf. Sci. 325 (1995) L421.
[9] S.M. Vesecky, X. Xu, D.W. Goodman, J. Vac. Sci. Technol. A 12 (1994) 2114.
[10] H. Schlichting, D. Menzel, Rev. Sci. Instrum. 64 (2013) 1993.
[11] V.P. Holbert, S.J. Garrett, J.C. Bruns, P.C. Stair, E. Weitz, Surf. Sci. 314 (1994) 107.
[12] P. Feulner, D. Menzel, J. Vac. Sci. Technol. A 17 (1980) 662.
[13] D. Cappus, PhD thesis, Ruhr-Universität Bochum, Bochum, Germany, 1995.
[14] R. Lindsay, P. Baumgärtel, R. Terborg, O. Schaff, A.M. Bradshaw, D.P. Woodruff, Phys. Rev. Lett., submitted for publication.
[15] R.W.G. Wyckoff, Crystal Structures, 2nd ed., Wiley Interscience, New York, 1965. vol. 1.

[16] E. Habenschaden, J. Küppers, Surf. Sci. 138 (1984) L147.
[17] H. Pfnür, P. Feulner, D. Menzel, J. Chem. Phys. 79 (1983) 4613.
[18] C.N. Chittenden, E.D. Pylant, A.L. Schwaner, J.M. White, Thermal desorption and mass spectrometry, in: A.T. Hubbard (Ed.), The Handbook of Surface Imaging and VisualizationCRC Press, Boca Raton, FL, 1995.
[19] P.A. Redhead, Vacuum 12 (1962) 203.
[20] P. Audibert, M. Sidoumou, J. Suzanne, Surf. Sci. 273 (1992) 467.
[21] S. Furuyama, H. Fujii, M. Kawamura, T. Morimotor, J. Phys. Chem. 82 (1978) 1028.
[22] M.A. Nygren, L.G.M. Pettersson, Z. Baraniarán, L. Seijo, J. Chem. Phys. 100 (2010) 1994.
[23] K.M. Neyman, S.Ph. Ruzankin, N. Roesch, Chem. Phys. Lett. 246 (1995) 546.
[24] L. Chen, R. Wu, N. Kioussis, Q. Zhang, Chem. Phys. Lett. 290 (1998) 255.
[25] J.-W. He, C.A. Estrada, J.S. Corneille, M.-C. Wu, D.W. Goodman, Surf. Sci. 261 (1992) 164.